5.3 PROBABILITY OF SIGNIFICANT CONVECTION BASED ON BLENDED FORECAST

Yin-lam NG*, On-pong CHEUNG, Ka-yee YIM, Christy Yan-Yu LEUNG, Mang-hin KOK

Hong Kong Observatory, Hong Kong, China

1. INTRODUCTION

The Hong Kong Observatory (HKO) has been blending extrapolated radar reflectivity with simulated reflectivity from numerical weather prediction (NWP) for significant convection nowcast and forecast up to 6 hours (Cheung et al. 2014), but the forecast was spatially limited to radar's coverage. HKO then explored utilising artificial neural network to convert multispectral imagery of Japan Meteorological Agency Himawari-8 Satellite into radar reflectivity (Woo et al. 2017; Leung et al. 2020). The satellite derived radar reflectivity (SDRR) made blending forecast for large area possible.

Section 2 described a seamless significant convection forecast based on SDRR and NWP reflectivity. Section 3 presented two types of significant convection probability forecast developed with their evaluation metrics and relevant case studies.

2. BLENDED FORECAST

2.1. Satellite nowcast

HKO has developed a suite of nowcasting systems, which has been known as the "Short-range Warning of Intense Rainstorms in Localized Systems" (SWIRLS), to aid rainstorm warning operation as well as high-impact weather forecasting for the public and the aviation community (WMO 2010; Woo et al. 2017; Cheung et al. 2014).

To extend the area coverage of this nowcasting system (Leung et al. 2020; Chan et al. 2021), HKO used artificial neural network (ANN) technique to simulate radar reflectivity from 7 spectral bands observed by the Advanced Himawari Imager (AHI) of the Japan Meteorological Agency (JMA) Himawari-8 (H-8) satellite. In addition, the ANN model was applied to observations by the GEO-KOMPSAT-2A (GK-2A) satellite of the Korea Meteorological Administration (KMA) to provide satellite derived radar reflectivity (SDRR) covering Central Asia and the Indian Ocean.

The SDRR by H-8, now Himawari-9 (H-9), and GK-2A would be extrapolated at 30-minute intervals for up to 8 hours by a semi-Lagrangian scheme along the optical flow motion vectors and is referred to as "extrapolated SDRR".

*Corresponding author address: Danice YL Ng, Hong Kong Observatory, 134A Nathan Road, Kowloon, Hong Kong, China.; E-mail: ylng@hko.gov.hk.

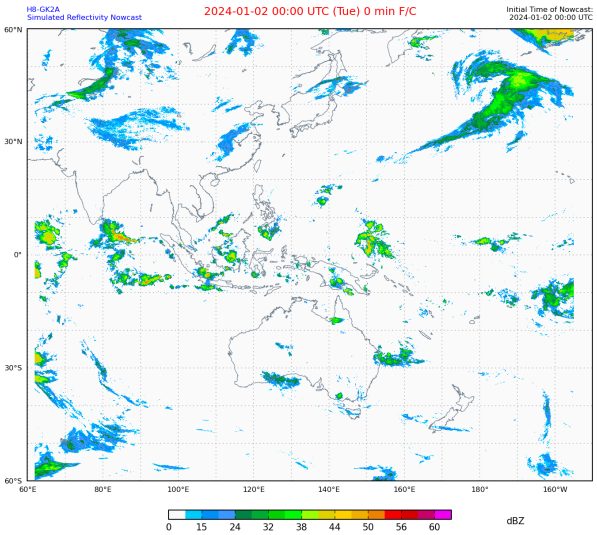

FIG. 1. Satellite derived radar reflectivity (SDRR) at 00 UTC on 02 January 2024.

2.2. Numerical Weather Prediction (NWP) model

Hourly precipitation from European Centre for Medium-Range Weather Forecasts (ECMWF) model was converted to radar reflectivity following a standard Marshall-Palmer (Marshall and Palmer 1948) $Z - R$ relation $Z = 200R^{1.6}$ in this study.

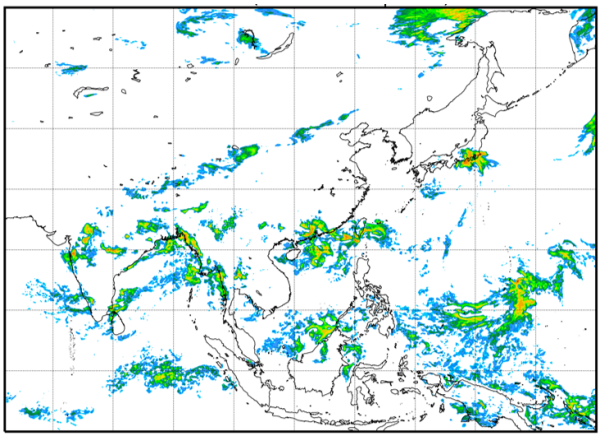

FIG. 2. Hourly precipitation forecast converted to radar reflectivity following a standard Marshall-Palmer $Z - R$ relation for 00 UTC on 8 September 2023 with ECMWF model initiated at 18 UTC on 7 September 2023.

The ECMWF has pioneered a system to predict forecast confidence, namely the Ensemble Prediction System (EPS). It comprises one control forecast (CNTL) plus 50 forecasts each with slightly altered initial conditions and slightly altered model physics. The horizontal resolution of the 51 forecasts is around 9 km (ECMWF 2023). Similar to NWP reflectivity used in the blended forecast, 3-hourly precipitation from ECMWF EPS was converted to radar reflectivity assuming uniform rainfall across the 3 hours and following a standard Marshall-Palmer $Z-R$ relation.

2.3. Blending satellite nowcast and NWP model

With reference to "Rainstorm Analysis & Prediction Integrated Data-processing System" (RAPIDS) (Li et al. 2005) that blends outputs from SWIRLS with NWP to generate an optimal Quantitative Precipitation Forecast (QPF) for operational guidance in rainstorm situations, HKO developed blending technique based on extrapolated SDRR and NWP radar reflectivity (Cheung et al. in preparation).

Based on fractional skill scores (FSS), optimal hourly weightings were chosen for T+1 hour to T+8 hours and were latitude dependent. Currently, optimal weightings for blending were selected based on trailing 12-month's performance to provide hourly gridded information on the presence and distribution of convective weather for the next 8 hours. The blended forecast information is radar reflectivity and being updated every hour.

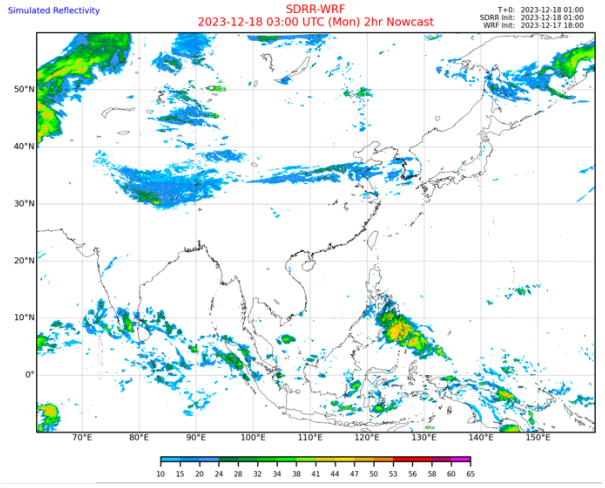

FIG. 3. Blended satellite derived radar reflectivity (SDRR) initialised at 01 UTC on 18 December 2023 for T+2 hours forecast (03 UTC on 18 December 2023).

3. PROBABILITY OF SIGNIFICANT CONVECTION

Two types of significant convection probability forecasts have been explored and details given in Sections 3.1 and 3.2 respectively. They were constructed such that they could quantify different forecast uncertainties.

Aligning with the convective weather definition used for blended forecast, convective weather probability is defined as the proportion of EPS-blended forecasts giving a forecast of greater than 33 dBZ.

3.1. Perturbing the blended weightings

Inspired by the idea of sensitivity analysis used in statistical modelling (Saltelli 2002), probability of significant convection based on different weightings (w=[0.0, 0.1, 0.2, ..., 0.8, 0.9, 1.0]) of blending SDRR with NWP reflectivity was explored. A range of weightings were used to study how extrapolated SDRR and NWP reflectivity might contribute to the uncertainty in the blended forecast. Two types of blending were explored: one with and one without Salience-Preserving Cross Dissolve (SalCD) (Hwang et al. 2015; Wang et al. 2015). Hwang et al. (2015) showed that SalCD that preserved the values in both the extrapolation and model forecasts if they are high enough would avoid the problem of every value being cut half in the linear cross dissolve method.

$$\text{dBZ}_{\text{without SalCD}} = w \times \text{dBZ}_{\text{nwp}} + (1-w) \times \text{dBZ}_{\text{sdrr}}$$

$$\text{dBZ}_{\text{SalCD blended}} = w_{SalCD} \times \text{dBZ}_{\text{nwp}} + (1-w_{SalCD}) \times \text{dBZ}_{\text{sdrr}}$$

$$w_{SalCD} = 0.5 \times \left[\frac{w \times I}{(w \times I)+(1-w)(1-I)} + \frac{\sqrt{w^2+I^2}}{\sqrt{w^2+I^2}+\sqrt{(1-w)^2+(1-I)^2}} \right]$$

where $I =$ cumulative density function of $(N_{nwp} - N_{sdrr})$. and N_{nwp}, N_{sdrr} are normalised intensity of NWP, SDRR respectively.

Three evaluation metrics were calculated for both blending methods (with or without SalCD): Averaged Fractions Skill Score (FSS), Brier Score, Continuous Ranked Probability Score (CRPS) for July to December 2023 and given in Figure 4.

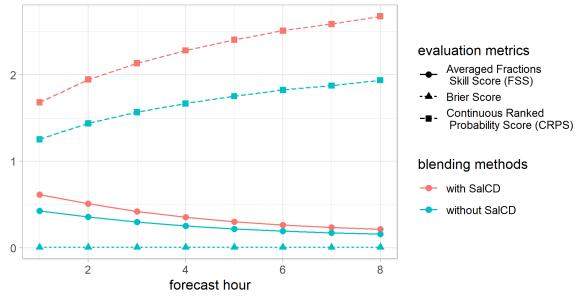

FIG. 4. Evaluation metrics for both blending methods plotted against forecast hour for July to December 2023.

Both methods showed better forecast skills at shorter forecast hours. Since significant convection would

occupy limited area over the whole forecast area and most places would not have significant convection, Brier Scores are always close to zero (both methods' Brier Scores near $y = 0$ as shown in Figure 4). For blending with SalCD, as it would preserve more significant convection (Figure 5), it has higher averaged FSS compared to blending without SalCD (Figure 6). In contrast, blending with SalCD has higher CRPS than blending without SalCD. However, over the verification area domain, many locations have no rainfall or light rainfall with dBZ<33, there was no closed form of CRPS available for this heavily tailed distribution. Therefore, based on both Brier Scores and average FSS, blending with SalCD would be better for probability forecast generation.

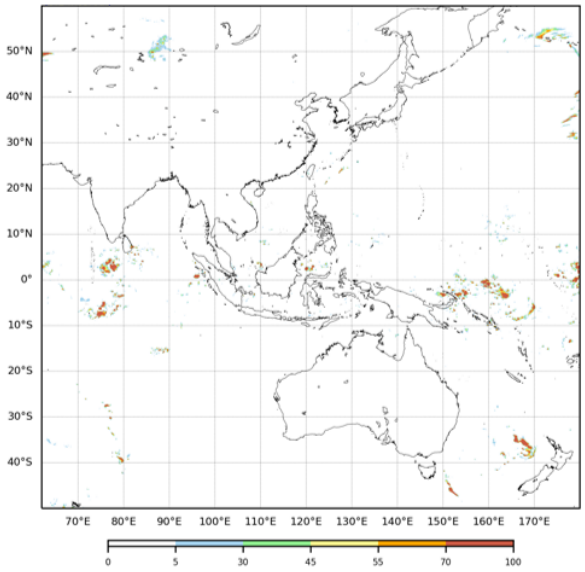

FIG. 5. Probability of ≥ 33 dBZ with SalCD initialised at 00 UTC on 28 December 2023 for T+1 hour forecast (01 UTC on 28 December 2023).

3.2. *Blending with ensemble forecast*

Optimal weightings used in blended forecast were not used in blending convective weather nowcast with ECMWF EPS. This is because optimal weightings would introduce much weightings in convective weather nowcast at small forecast hours, and limit the capability of blended EPS forecast to quantify forecast uncertainty.

Linear increasing weightings were used to conserve the higher forecast skill in convective weather nowcast at small forecast hours (Figure 7) while allowing ECMWF EPS to provide forecast spread, especially in longer forecast hours (Figure 8). The set of extrapolated SDRR is blended with individual member of the ECMWF EPS to construct a cluster of 51 EPS-blended forecasts. Weightings between extrapolated SDRR and ECMWF

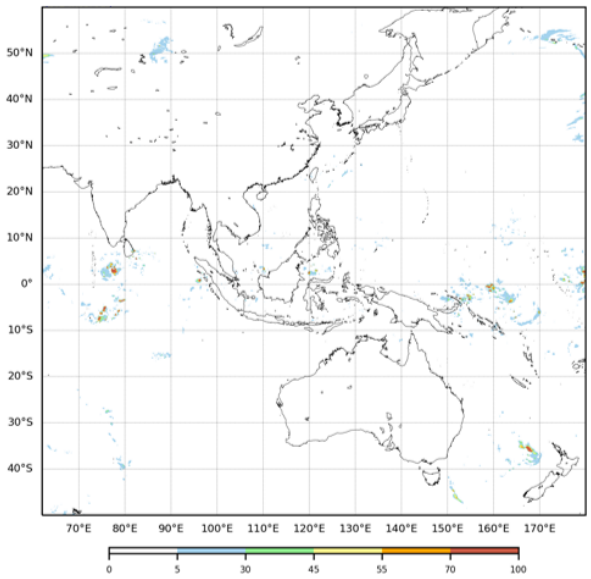

FIG. 6. Probability of ≥ 33 dBZ without SalCD initialised at 00 UTC on 28 December 2023 for T+1 hour forecast (01 UTC on 28 December 2023).

EPS members were set to be 10% model at T+1, 20% model at T+2, …, 80% model at T+8. Blending with SalCD is essential, otherwise, the spread introduced by blending with ECMWF EPS would lead to nearly all zero probability forecast, which would be useless in operation. Because when the problem of every value being cut half without SalCD is introduced in each blending with ECMWF EPS member, the probability of ≥ 33 dBZ would become so low at each grid point.

As ECMWF EPS tried to capture a wide range of possible future states of the atmosphere, probability space spanned by blending with ECMWF EPS member would be larger than that spanned by perturbing blending weights between SDRR and deterministic NWP.

4. EXAMPLE

A trough of low pressure associated with the remnants of Tropical Cyclone Haikui brought prolonged torrential rain to Hong Kong on 7 and 8 September 2023 (HKO 2023). During the torrential rain episode, the HKO Headquarters registered a record-breaking hourly rainfall of 158.1 mm from 15 UTC to 16 UTC on 7 September, the highest since records began in 1884.

Without taking nowcast into consideration, the probability for significant convection (≥ 33 dBZ) derived from 3-hourly rainfall by ECMWF EPS in the vicinity of Hong Kong was rather low (Figures 9 and 10).

By blending the latest convection nowcast with members of ECMWF EPS, the probability of significant convection provided better heads-up for forecasters that convection might be stickier than model forecast. The

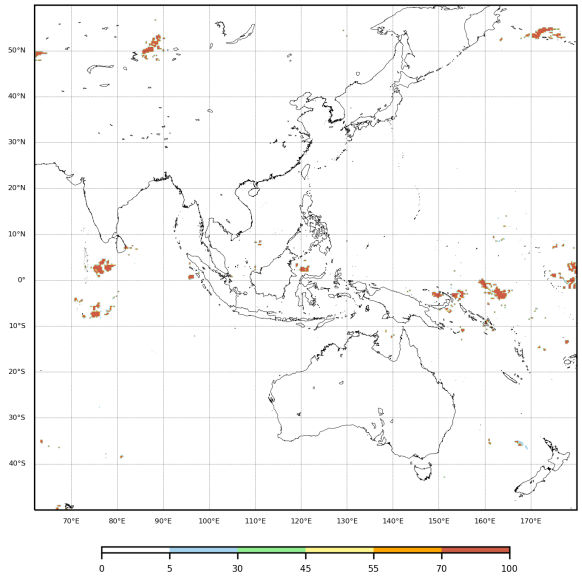

FIG. 7. Probability of ≥ 33 dBZ given by EPS-blended forecasts with SalCD initialised at 00 UTC on 28 December 2023 for T+1 hour forecast (01 UTC on 28 December 2023).

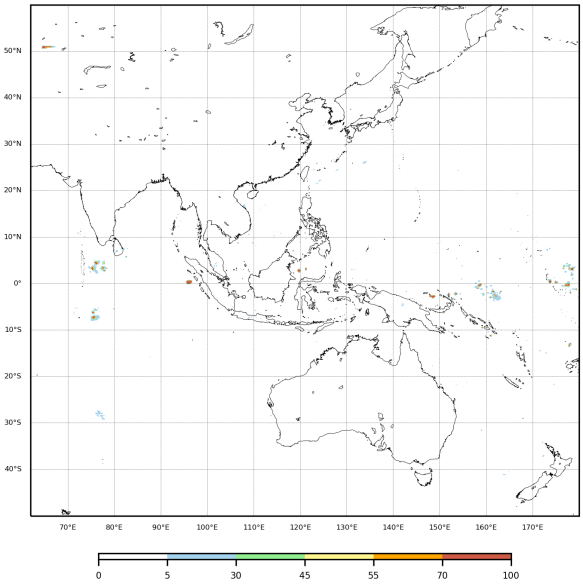

FIG. 8. Probability of ≥ 33 dBZ given by EPS-blended forecasts with SalCD initialised at 00 UTC on 28 December 2023 for T+8 hour forecast (08 UTC on 28 December 2023).

probability remained high in the vicinity of Hong Kong given by blended ensemble forecast initialised at 15 UTC on 7 September 2023 for forecast hour T+1 in Figure 11 till T+8 in Figure 18.

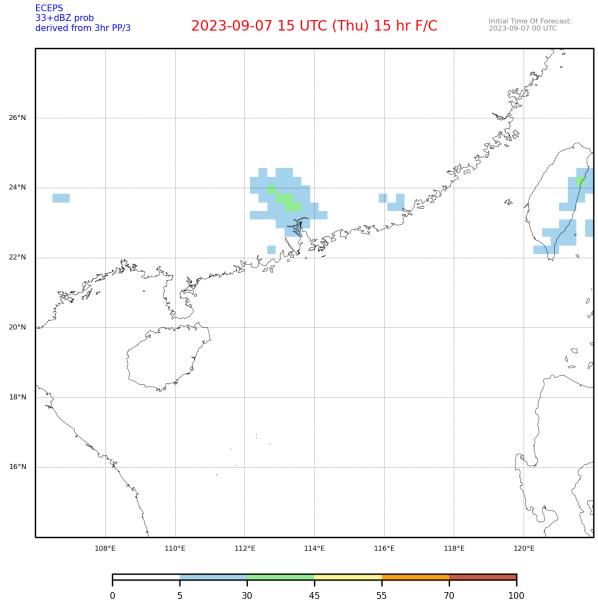

FIG. 9. Probability of ≥ 33 dBZ among ECMWF EPS initialised at 00 UTC on 7 September 2023 for T+15 hour forecast (15 UTC on 7 September 2023).

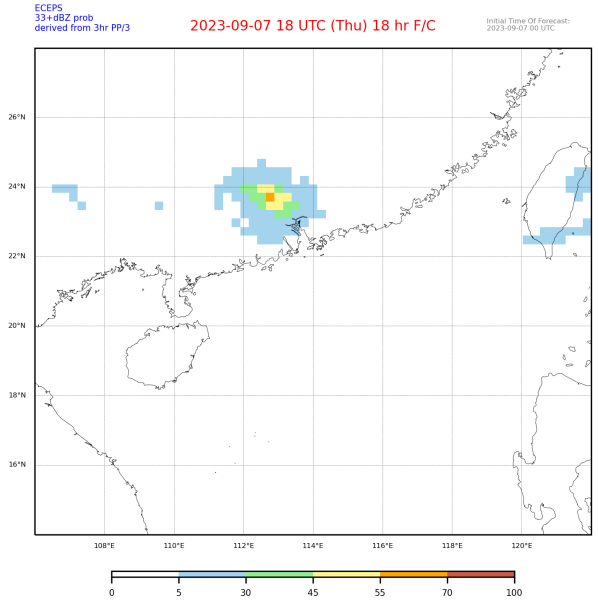

FIG. 10. Probability of ≥ 33 dBZ among ECMWF EPS initialised at 00 UTC on 7 September 2023 for T+18 hour forecast (18 UTC on 7 September 2023).

5. DISCUSSION

As part of the World Weather Research Programme (WWRP) led by the WMO Research Board, Aviation Research and Development Project (AvRDP) is a project that focuses on scientific advancement and capacity development in aeronautical observation, forecasting,

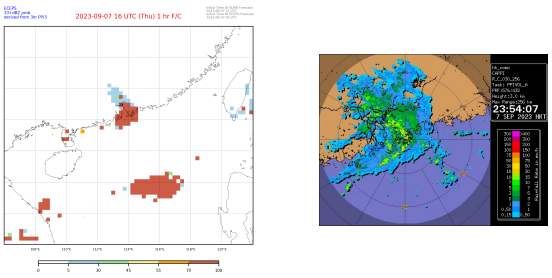

FIG. 11. (Left) Probability of ≥ 33 dBZ among nowcast blended ECMWF EPS initialised at 15 UTC on 7 September 2023 for T+1 hour forecast (16 UTC on 7 September 2023); (Right) HKO 512 km radar observation at 15:54:07 UTC on 7 September 2023.

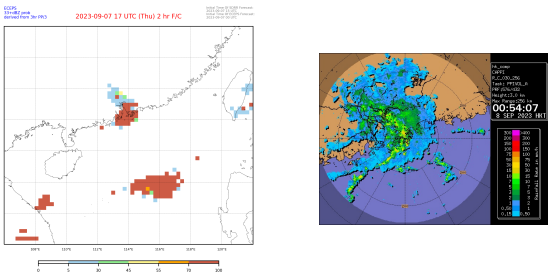

FIG. 12. (Left) Probability of ≥ 33 dBZ among nowcast blended ECMWF EPS initialised at 15 UTC on 7 September 2023 for T+2 hour forecast (17 UTC on 7 September 2023); (Right) HKO 512 km radar observation at 16:54:07 UTC on 7 September 2023.

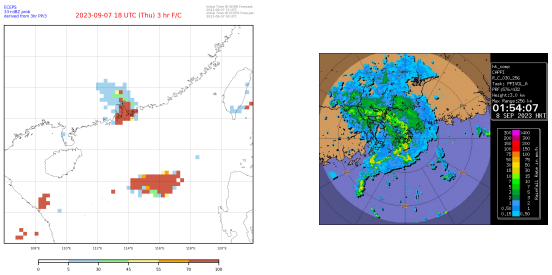

FIG. 13. (Left) Probability of ≥ 33 dBZ among nowcast blended ECMWF EPS initialised at 15 UTC on 7 September 2023 for T+3 hour forecast (18 UTC on 7 September 2023); (Right) HKO 512 km radar observation at 17:54:07 UTC on 7 September 2023.

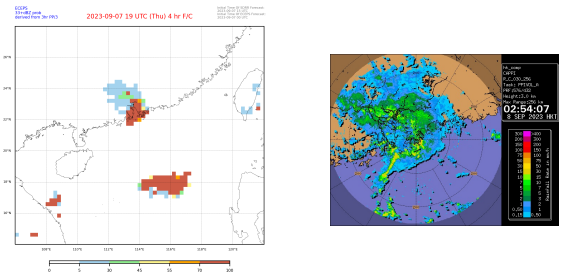

FIG. 14. (Left) Probability of ≥ 33 dBZ among nowcast blended ECMWF EPS initialised at 15 UTC on 7 September 2023 for T+4 hour forecast (19 UTC on 7 September 2023); (Right) HKO 512 km radar observation at 18:54:07 UTC on 7 September 2023.

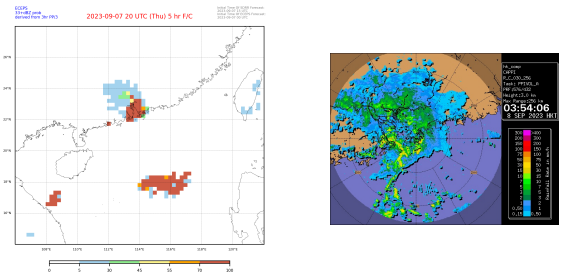

FIG. 15. (Left) Probability of ≥ 33 dBZ among nowcast blended ECMWF EPS initialised at 15 UTC on 7 September 2023 for T+5 hour forecast (20 UTC on 7 September 2023); (Right) HKO 512 km radar observation at 19:54:06 UTC on 7 September 2023.

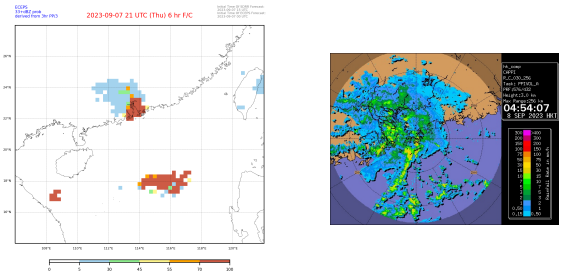

FIG. 16. (Left) Probability of ≥ 33 dBZ among nowcast blended ECMWF EPS initialised at 15 UTC on 7 September 2023 for T+6 hour forecast (21 UTC on 7 September 2023); (Right) HKO 512 km radar observation at 20:54:07 UTC on 7 September 2023.

and warning of significant convection and associated hazards.

The first phase of the AvRDP (WMO 2019) focused on nowcasting aviation weather over the Terminal Control Area for the next 0-6 hours. AvRDP-2 (WMO 2023) is the second phase (2021-2025) of AvRDP and will study the blending of nowcasting information.

HKO is taking part in AvRDP-2 and has planned to demonstrate benefits of blended significant convection forecast for supporting gate-to-gate operation. In particular, hazardous weather encounter statistics based on blended significant convection forecast would be provided to airlines for their trial and feedback.

At the second AvRDP-2 Scientific Steering Committee meeting in September 2023, members agreed on investigating probabilistic information for flight planning (Wigniolle et al. 2023). This study showed two ways of generating significant convection forecast: (i) perturbing

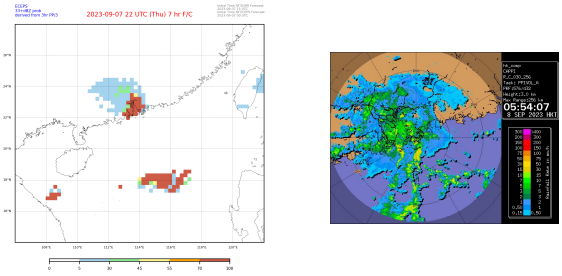

FIG. 17. (Left) Probability of ≥ 33 dBZ among nowcast blended ECMWF EPS initialised at 15 UTC on 7 September 2023 for T+7 hour forecast (22 UTC on 7 September 2023); (Right) HKO 512 km radar observation at 21:54:07 UTC on 7 September 2023.

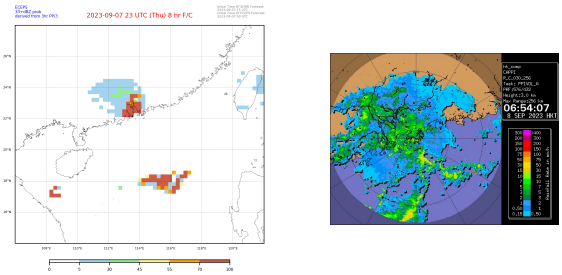

FIG. 18. (Left) Probability of ≥ 33 dBZ among nowcast blended ECMWF EPS initialised at 15 UTC on 7 September 2023 for T+8 hour forecast (23 UTC on 7 September 2023); (Right) HKO 512 km radar observation at 22:54:07 UTC on 7 September 2023.

the blending weights; and (ii) blending nowcast with NWP ensemble members. These probabilities would be able to provide forecast uncertainty associated with blended significant convection forecast. Noting the value added with probabilities available, verification of these probabilities and application of these probabilities on generating hazardous weather encounter statistics for aviation users will be explored.

Acknowledgments. Great appreciation to all pilots and airline staff who have provided inputs and comments regarding hazardous weather encounter statistics. Special thanks to the staff of the International Aviation Meteorological Collaboration Division in HKO for their valuable comments and technical support.

REFERENCES

Chan, W. S., C. Y. Y. Leung, and P. W. Li, 2021: Enhancement of the hko satellite derived radar reflectivity algorithm in recognition of significant convection. *The 26th Guangdong - Hong Kong - Macao Meeting on Cooperation in Meteorological Operations*.

Cheung, O. P., Y. Y. Leung, Y. L. Ng, M. H. Kok, and S. T. Chan, in preparation: Seamless significant convection forecast for aviation by blending satellite nowcast with numerical weather prediction.

Cheung, P., P. W. Li, and W. K. Wong, 2014: Blending of extrapolated radar reflectivity with simulated reflectivity from nwp for a seamless significant convection forecast up to 6 hours. *17th Conference on Aviation, Range, and Aerospace Meteorology*.

ECMWF, 2023: Model upgrade increases skill and unifies medium-range resolutions. URL https://www.ecmwf.int/en/newsletter/176/earth-system-science/ifs-upgrade-brings-many-improvements-and-unifies-medium.

HKO, 2023: The weather of september 2023. URL https://www.hko.gov.hk/en/wxinfo/pastwx/mws2023/mws202309.htm.

Hwang, Y., A. J. Clark, V. Lakshmanan, and S. E. Koch, 2015: Improved nowcasts by blending extrapolation and model forecasts. *Weather and Forecasting*, **30 (5)**, 1201–1217.

Leung, C. Y. Y., H. C. Tam, W. S. Chan, and H. K. Fok, 2020: Development of satellite-based cloud top height and convection nowcasting products in support of sigmet coordination in apac region. *100th American Meteorological Society Annual Meeting*, AMS.

Li, P. W., W. K. Wong, and E. S. T. Lai, 2005: Rapids—a new rainstorm nowcasting system in hong kong. *Proceeding, WWRP Symposium on Nowcasting and Very Short Range Forecasting*, 7–17.

Marshall, J. S., and W. M. K. Palmer, 1948: The distribution of raindrops with size. *Journal of Atmospheric Sciences*, **5 (4)**, 165–166.

Saltelli, A., 2002: Sensitivity analysis for importance assessment. *Risk analysis*, **22 (3)**, 579–590.

Wang, G., W.-K. Wong, Y. Hong, L. Liu, J. Dong, and M. Xue, 2015: Improvement of forecast skill for severe weather by merging radar-based extrapolation and storm-scale nwp corrected forecast. *Atmospheric Research*, **154**, 14–24.

Wigniolle, S., C. Davis, and P. Buchanan, 2023: Outcomes of the second meeting of the aviation research and development project phase 2 scientific steering committee. URL https://community.wmo.int/en/activity-areas/aviation/resources/newsletters/2023-2#avrdp2-ssc-2.

WMO, 2010: *Manual on the Global Data-processing and Forecasting System*. World Meteorological Organization.

WMO, 2019: Aviation research and development project. URL https://avrdp.hko.gov.hk/.

WMO, 2023: Aviation research and development project phase 2. URL https://avrdp.hko.gov.hk/Phase2/index.html.

Woo, W. C., Y. Y. Ip, W. K. Wong, and N. H. Chan, 2017: Development of satellite reflectivity retrieval

technique for tropical cyclone rainfall nowcasting. *Fourth International Workshop on Tropical Cyclones Landfall Processes (IWTCLP-4)*, 5–7.